

Evaluation of Pure-Component Adsorption Properties of Silicalite Based on the Langmuir and Sips Models

Alessio Caravella and Pasquale F. Zito

Dept. of Environment and Chemical Engineering, The University of Calabria, Via Pietro Bucci, Cubo 44A, 87036 Rende (CS), Italy

Adele Brunetti and Giuseppe Barbieri

Institute on Membrane Technology (ITM-CNR), National Research Council, Via Pietro Bucci, Cubo 17C, 87036 Rende (CS), Italy

Enrico Drioli

Dept. of Environment and Chemical Engineering, The University of Calabria, Via Pietro Bucci, Cubo 44A, 87036 Rende (CS), Italy

Institute on Membrane Technology (ITM-CNR), National Research Council, Via Pietro Bucci, Cubo 17C, 87036 Rende (CS), Italy

DOI 10.1002/aic.14925

Published online July 14, 2015 in Wiley Online Library (wileyonlinelibrary.com)

The Langmuir and Sips models parameters were estimated for the adsorption of several light gases and hydrocarbons (H_2 , CH_4 , CO_2 , CO , N_2 , C_2H_6 , C_3H_8 , $n-C_4H_{10}$) in silicalite along with their functionality with temperature. This is a scientific attempt to resume and reconcile the number of available experimental data and supply scientists and other operators with the adsorption properties of silicalite within a wider range of temperature and pressure. Furthermore, to provide readers with more detailed information on where each of the two models work better, the analysis is divided into three temperature ranges: low-temperature, high-temperature, and whole temperature range. As a result, it is found that the Langmuir model works well in the whole temperature range for the light gases considered but not for the other hydrocarbons, for which it is better to use the Sips model by splitting calculation over low- and high-temperature range.

© 2015 American Institute of Chemical Engineers AIChE J, 61: 3911–3922, 2015

Keywords: silicalite, zeolite, membranes, adsorption properties, gas separation

Introduction

Adsorption is crucial to study the catalytic characteristics of various materials. Furthermore, unit operations based on adsorption are successfully used to purify gas streams. Species separation through adsorption is mainly driven by three different mechanisms: steric, equilibrium, and kinetic. The steric mechanism is based on the pores dimension, as it allows just small molecules to enter. The equilibrium mechanism is based on the solid capability to accommodate different species with different extent. Finally, the kinetic one is based on the different rates of diffusion into the pores.¹

For an efficient separation, a good choice is generally to use adsorbents with good adsorptive capacity and fast kinetics, this allowing a shorter residence time in the purification column and/or a small amount of adsorbent required. Some important adsorbents used in industry are alumina, silica gel,

activated carbon, and zeolites, which are alumino-silicate with channel size in the range of molecular size (3–10 Å).^{2,3}

In the present study, the considered zeolite is the silicalite, which belongs to MFI-type (mordenite framework inverted) zeolite, composed by orthorhombic cells with the following dimensions: $a = 20.07$ Å, $b = 19.92$ Å, $c = 13.42$ Å.^{3–7}

The MFI membranes are widely studied for gas separation, in particular for CO_2/N_2 and CO_2/CH_4 separation.⁸ For example, Lovallo et al.⁹ reported the gas performances on MFI membrane. The results of single gas measurements show an ideal selectivity for H_2/N_2 and H_2/CH_4 higher than 30 at 125°C, whereas CO_2/CH_4 and O_2/N_2 are 8 and 3, respectively. Single and binary permeation of CH_4 and CO_2 across silicalite-1 was also investigated by Zhu et al.¹⁰ who provide an ideal CO_2/CH_4 selectivity that decreases with increasing both feed pressure and temperature. The maximum value is around 4 at 303 K and 101.3 kPa.

Along with experimental studies, several modeling and simulation works were also performed^{4,6–19} with the aim at better characterizing the single-species adsorption properties of silicalite.

Both definition and characterization of the adsorption properties strongly depend on the adsorption model used for the

Additional Supporting Information may be found in the online version of this article.

Correspondence concerning this article should be addressed to G. Barbieri at g.barbieri@itm.cnr.it.

© 2015 American Institute of Chemical Engineers

Table 1. An Overview of the Operating Conditions Ranges of the Published Experimental Isotherms Used in the Present Work

Species	Temperature Range	Temperature Interval (K)	P_{maximum} (kPa)	References	Number of Isotherms
H ₂	Low	—	—	—	—
	High	—	—	—	—
	Whole	305–343	1483	11	2
CH ₄	Low	275–304	2052	11–13,15,16,18	8
	High	308–408	2072	11–13,15,16,18	11
	Whole	275–408	2072	11–13,15,16,18	19
CO ₂	Low	277–305	2001	11,12,15,18	5
	High	308–408	2044	10–12,15,17,18	11
	Whole	277–408	2044	10–12,15,17,18	16
CO	Low	—	—	—	—
	High	—	—	—	—
	Whole	305–341.5	744	11	2
N ₂	Low	288–305	1000	11,15,18	4
	High	313–345	1000	11,15,18	4
	Whole	288–345	1000	11,15,18	8
C ₂ H ₆	Low	273–300	2109	12–15	7
	High	308–473	2058	6,12–15	11
	Whole	273–473	2109	6,12–15	18
C ₃ H ₈	Low	273–303	538	6,12–14	6
	High	308–473	805	6,12–14	10
	Whole	273–473	805	6,12–14	16
C ₄ H ₁₀	Low	275–303	190	6,12,13	4
	High	308–473	190	6,12,13	9
	Whole	275–473	190	6,12,13	13

analysis. The Langmuir approach provides properties of adsorption averaged over a complex surface, with the aim at simplifying the analysis and obtaining values suitable to be directly used by scholars and researchers.

Starting from his approach, many others have been developed aimed at taking into account more detailed complexities. For example, the Sips model accounts for the effect of lateral interactions among adsorbed molecules by introducing a pressure exponent in the adsorption isotherm, changing in this way the form of the Langmuir one (see Eqs. 1–7).¹

These models have the advantage to be relatively easy by taking into account, at the same time, the main phenomena involved in the monolayer adsorption.

Concerning silicalite, although number of extensive studies reporting its physicochemical and adsorption properties present in the open literature,^{4,6–18} in Authors' opinion there is a lack of systematicity in both determining and using the considerable amount of available experimental data. This is owing to the fact that the majority of results obtained by each research group seem to be evidently not related to each other, each of them being in practice unlinked with others of the same type. This is a strong limitation for a user who wants to have a clear and synthetic outline of such a complex situation.

In this context, the overall aim of the present work is to cover such a lack of systematicity by providing an overall reconciliation of the available and coherent experimental data from the literature.

Table 1 reports all the adsorption isotherms (a total of 94 isotherms over eight gas species) considered in this work and the corresponding temperature and pressure range.

To our intention, these isotherms should be as representative as possible of all the operating conditions ranges considered in the open literature. Furthermore, empirical functionalities with temperature (see Eqs. 8 and 9) are considered within different temperature ranges to provide a quantification of the temperature influence on adsorption parameters like saturation loading and lateral interactions exponent, this further enlarging the validity of the present investigation.

To carry out our investigation, the experimental isotherms obtained in the single literature works are included in a wider systematic procedure allowing a reconciliation of the analyzed data within a clearer context, which in turn allows a simpler recognition and usage of the adsorption parameters. However, as in most cases the pretreatment and post-treatment to which the zeolites are subjected are not fully known, the strong dependency of the adsorption properties on them cannot be fully understood.

The choice of the experimental data used for regression deserves some explanations. As mentioned above, we collect a number of experimental data to carry out our study. However, it is not generally known and clear *a priori* which set of data are suitable for analysis, as some data could be “not coherent” to each other. In our investigation, it is decided that a subset of data (i.e., a group of isotherms) is not coherent when it is in contrast with the majority of the available data. In practice, having a set of isotherms, we consider coherent a subset of isotherms whose temperature continuously increases with increasing loading for a fixed pressure.

Mathematical Approach

Adsorption models

As aforementioned, all the experimental data considered in this article are fitted according to the Langmuir and Sips adsorption models. The former is chosen because it is largely used in the literature, whereas the latter because of the simplicity in taking into account the molecule-molecule lateral interactions. The Langmuir model is given by Eqs. 1–4

$$C_{\mu} = C_{\mu s} \frac{b_{\text{Lang}} P}{1 + b_{\text{Lang}} P} \quad (1)$$

$$b_{\text{Lang}} = b_{\infty, \text{Lang}} e^{\left(\frac{Q_{\text{Ads, Lang}}}{R_g T} \right)} \quad (2)$$

$$b_{\infty, \text{Lang}} = \frac{b_0}{\sqrt{T}} \quad (3)$$

$$b_0 = \frac{a}{k_{\text{dso}} \sqrt{2\pi MR_g}} \quad (4)$$

whereas the Sips one is given by Eqs. 5–7

$$C_{\mu} = C_{\mu s} \frac{(b_{\text{Sips}} P)^{\frac{1}{n}}}{1 + (b_{\text{Sips}} P)^{\frac{1}{n}}} \quad (5)$$

$$b_{\text{Sips}} = b_{0, \text{Sips}} \exp \left[\frac{Q_{\text{Ads, Sips}}}{RT} \right] \quad (6)$$

$$b_{0, \text{Sips}} = b_{\infty, \text{Sips}} \exp \left[-\frac{Q_{\text{Ads, Sips}}}{RT_0} \right] \quad (7)$$

The parameter b , present in both the expressions of Langmuir and Sips models, is the so-called “affinity constant,” indicating the adsorption strength of an adsorbate molecule onto a surface,¹ whereas b_0 is the parameter of the desorption kinetics.

The semiempirical parameter n appearing in Eq. 5 indicates the system heterogeneity and, generally, is greater than unity. When n is equal to unity, the Sips equation reverts to the Langmuir one. To measure the temperature dependence of n and saturation loading, the following empirical expressions are chosen, which are not originally part of the two adsorption models¹

$$\frac{1}{n} = \frac{1}{n_0} + \alpha \left[1 - \frac{T_0}{T} \right] \quad (8)$$

$$C_{\mu s} = C_{\mu s0} e^{\left[\chi \left(1 - \frac{T_0}{T} \right) \right]} \quad (9)$$

Equation 9 states that the higher the temperature is, the lower the saturation loading. The magnitude of the parameter χ gives the temperature dependence of saturation loading.

However, in the case of the Langmuir model, some explanations are required concerning the form of Eq. 9. To do that, let us remind the definition of isosteric heat of adsorption (Q_{Iso}), which is generally defined as the ratio of the infinitesimal variation of the adsorbate enthalpy to the infinitesimal variation of the amount adsorbed (van’t Hoff equation, Eq. 10)¹

$$Q_{\text{Iso}} = -\Delta \tilde{H}_{\text{Iso}} = R_g T^2 \left(\frac{\partial \ln P}{\partial T} \right)_{C_{\mu}} \quad (10)$$

where ΔH_{Iso} is the molar isosteric enthalpy of adsorption. Using Eqs. 1–4 in Eq. 10, it is possible to demonstrate that, after some algebra, the following expression is obtained relating heat of adsorption ($Q_{\text{Ads, Lang}}$) and isosteric heat of adsorption ($Q_{\text{Iso, Lang}}$)

$$Q_{\text{Iso, Lang}} = \frac{R_g T}{2} + Q_{\text{Ads, Lang}} + \frac{\chi R_g T^2}{T_0(1-\theta)} \quad (11)$$

However, as also pointed out in the literature,¹ the third term goes toward infinity for θ approaching to the unity. The only way to avoid this behavior, which is not physically acceptable, is to set the parameter χ to zero, which implies a temperature-independent saturation loading.

Furthermore, considering that the first term is generally small compared with the second one ($Q_{\text{Ads, Lang}}$)—in most literature works $b_{\infty, \text{Lang}}$ is even considered constant with temperature (see, e.g., Bakker et al.²⁰)—it can be stated with a

sufficiently good approximation that isosteric heat of adsorption and heat of adsorption are basically equal in the Langmuir model. Therefore, according to Eq. 11, the Langmuir model cannot be used to estimate the isosteric heat of adsorption at values of loading approaching to the unity.

As well, also the Sips model shows the same consistency problem, shown from the relationship between heat of adsorption ($Q_{\text{Ads, Sips}}$) and isosteric heat of adsorption ($Q_{\text{Iso, Sips}}$) provided by Eqs. 12 and 13

$$Q_{\text{Iso, Sips}} = Q_{\text{Ads, Sips}} - \alpha R T_0 n^2 \ln \left[\frac{C_{\mu}}{C_{\mu s} - C_{\mu}} \right] + n \frac{\chi R_g T^2}{T_0} \left[\frac{C_{\mu s}}{C_{\mu s} - C_{\mu}} \right] \quad (12)$$

$$Q_{\text{Iso, Sips}} = Q_{\text{Ads, Sips}} - \alpha R T_0 n^2 \ln \left[\frac{\theta}{1-\theta} \right] + n \frac{\chi R_g T^2}{T_0} \left[\frac{1}{1-\theta} \right] \quad (13)$$

From these expressions, it can be easily observed that, when the parameter α approaches to zero (i.e., n approaches to the unity), the expression of the Sips isosteric heat of adsorption coincides with the Langmuir one, as expected. Moreover, if the functionality with temperature can be neglected (i.e., $\chi \approx 0$), the Sips heat of adsorption coincides with the isosteric heat of adsorption calculated at a fractional loading of 0.5.¹

Analogously to what seen for the Langmuir model, also the Sips one cannot be satisfactorily used for estimating the isosteric heat of adsorption for loading values approaching to the unity. However, although both models suffer for such a consistency problem, the average procedure used in this article (see discussion related to Eqs. 14–16) shows that a sufficiently good estimation is obtained using Eqs. 11 and 13.

Regression settings and remarks

A multivariate nonlinear regression was performed to evaluate the adsorption parameters. In particular, for each species, all the available isotherms were fitted at once with both Langmuir and Sips model, using the least squares method. For this purpose, the minimization routine already available in MATLAB[®] environment (namely “*lsqcurvefit*”) is used.²¹

However, owing to the number of parameters (four parameters in the Langmuir model and six parameters in the Sips one), a particular attention was paid to assuring that the minima of the objective function found by the routine were global minima and not local ones. To do that, the routine run 40 times using different initial guess values, which were changed according to a criterion for which, once the routine had provided an optimum set of parameter values, such a set was modified by changing randomly all values and providing the new set of input initial guess for the successive run. The relative normalized tolerance for the convergence condition was set to 10^{-8} for all runs.²¹

Results and Discussion

As the main objective of this work is to provide end users with actual values of adsorption parameters, the obtained results are presented in terms of both calculated isotherms, bar figures and tables, where the complete set of calculated parameters can be found (see Supporting Information).

Furthermore, to provide more specific pieces of information to scientists and researchers and to show them in which conditions the two models work better, the calculation is performed considering three temperature ranges: the whole temperature range, the low-temperature range, and the high-temperature one.

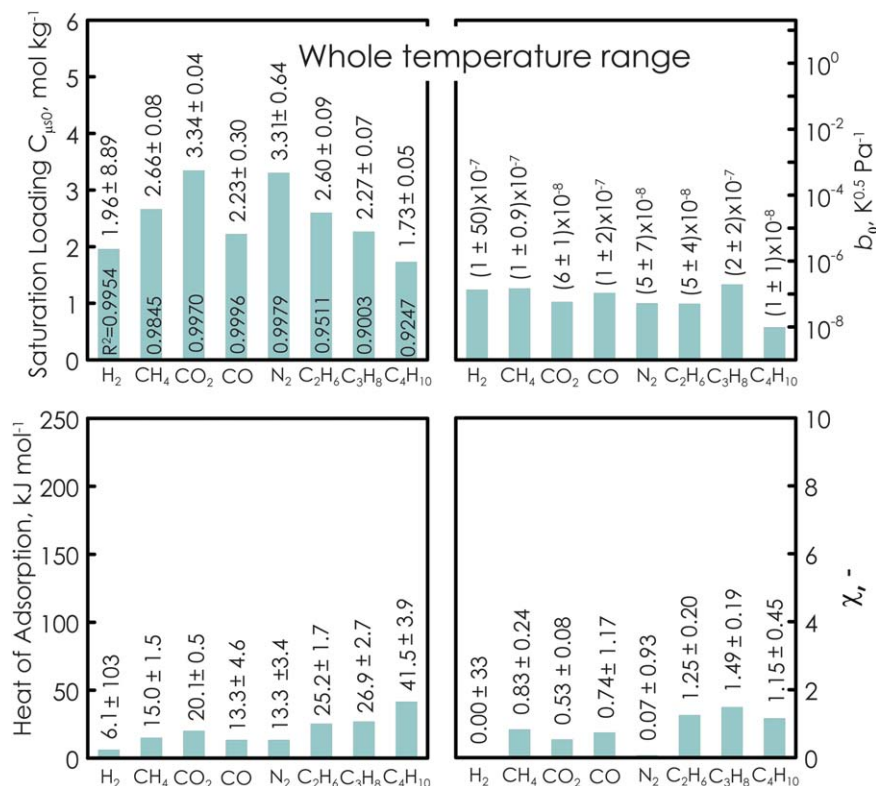


Figure 1. Calculated optimal values of the Langmuir model for the considered species.

Saturation loading $C_{\mu s0}$, parameter b_0 , heat of adsorption $Q_{Ads,Lang}$, empirical parameter χ . Whole temperature range (see Table 1). [Color figure can be viewed in the online issue, which is available at wileyonlinelibrary.com.]

In practice, first the multivariate regression is applied to all the available isotherms at once. Then, the whole temperature range is divided into two subranges (low- and high-temperature range) with the criterion that the former spans from the lowest temperature considered for each species up to the room temperature (around 295–303 K), whereas the latter spans from the temperature just higher than the room temperature to the maximum temperature considered.

Such an analysis arises from the consideration that the lower the temperature, the stronger the species-zeolite interaction. Therefore, at lower temperature, it is possible that simple adsorption models like the Langmuir one do not satisfactorily describe the macroscopic behavior of the adsorbed molecules.

Estimation of adsorption parameters: Whole temperature range

Figure 1 shows the optimal values of the adsorption properties in terms of parameters of the Langmuir model calculated for all species in the whole respective temperature ranges. As for the saturation loading, quite narrow confidence intervals are calculated for each component except H₂, this being a measure of the sensitivity of the obtained results to the initial guess.

Concerning H₂, relatively large confidence intervals are found with respect to the other components also for the other parameters, this generally indicating a higher calculation uncertainty. This fact is associated to the weakness of the hydrogen-zeolite physical bond, which makes the final parameter value strongly dependent on the initial guesses.

However, it must be also considered that the meaning of the confidence interval in being a measure of the calculation uncertainty loses its validity with the calculated optimal val-

ues approaching to zero, because every interval value is infinitely larger with respect to zero independently of the interval value. This means that in the Langmuir model there is no need to include the functionality of the H₂ saturation loading with temperature, which implies to set a priori the χ value of H₂ to zero.

Concerning the values of the determination coefficient R^2 for the Langmuir model, they are pretty satisfactory for all species except for the hydrocarbons (C₂H₆, C₃H₈, and C₄H₁₀), which shows values below around 0.95. As for the Sips model, R^2 is always higher than around 0.94. This fact, which basically depends on the higher number of parameters in the Sips model, suggests that this model is able to describe the adsorption behavior of the considered hydrocarbons more than the Langmuir one. As for the other species, it can be said that both models can be satisfactorily used.

Another important aspect to be considered is that, for the light gases but hydrogen and methane, the number of used literature references and the relatively high values of R^2 indicate that the sensitivity of the adsorption properties to the zeolites fabrication method is relatively small, contrarily to what is found for the hydrocarbons, for which the fabrication method seems to play a significant role.

As regards the temperature effect on saturation loading, which directly depends on the empirical parameter χ (Eq. 9), an interesting results obtained from simulation is that the saturation loadings of both H₂ and N₂ are forecast to be practically independent of temperature. However, in the case of H₂, the saturation loading presents a confidence interval that makes the calculation result pretty unreliable. Therefore, it is not possible to say that the H₂ saturation loading is independent of temperature just from this calculation.

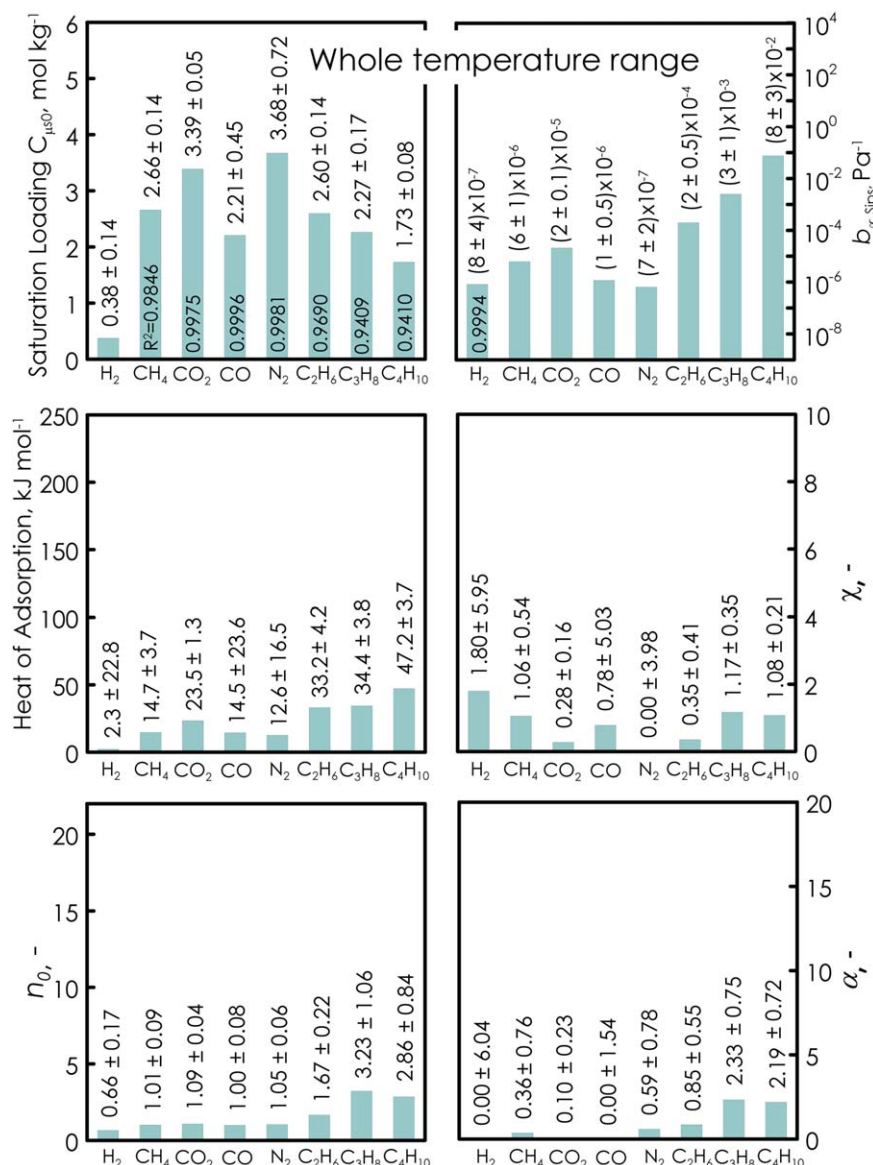


Figure 2. Calculated optimal values of the Sips model for the considered species.

Saturation loading $C_{\mu s0}$, Sips affinity constant at infinite temperature $b_{\infty,Sips}$, heat of adsorption $Q_{Ads,Sips}$, empirical parameter χ , empirical exponent n_0 , empirical parameter α . Whole temperature range (see Table 1). [Color figure can be viewed in the online issue, which is available at wileyonlinelibrary.com.]

A proof of that is given by the regression results using the Sips model (Figure 2), showing an optimal value for H₂ (1.80) that is sensibly higher than zero with a corresponding confidence interval being three times higher than the optimal value itself (5.95) although much less than that obtained from the Langmuir model. Differently, based on the results from the Sips model, the N₂ saturation loading is confirmed to be practically independent of temperature.

As for the other species, Figure 2 shows that the values of the saturation loading at the reference temperature ($C_{\mu s0}$) obtained with the Sips model are practically the same as those obtained with the Langmuir one, this implying that the values can be considered highly reliable.

Concerning the relationship between heat of adsorption ($Q_{Ads,Sips}$) and isosteric heat of adsorption ($Q_{Iso,Sips}$) based on the Sips model, the difference between the two quantities basically depends on just two parameters: α and n_0 (Eqs. 12 and 13), as the exponent n is a function of α and n_0 as well. The

former quantifies the strength of the functionality of the lateral interactions with temperature, whereas the latter represents the “degree” of interaction among the adsorbed molecules. In the case of both weak lateral interactions (n_0 close to the unity) and weak functionality of the lateral interactions with temperature (α close to zero), the Sips model approaches the Langmuir one and, thus, both models provide similar results.

This situation is depicted in Figure 3b, which shows a calculation example showing that the isosteric heat of adsorption for CO₂ is practically independent of temperature and has a similar behavior as the heat of adsorption, whereas the same does not occur for C₂H₆ (Figure 3a). This is owing to the very low value of parameter α (~ 0.1), which makes n very close to n_0 (Eq. 8).

By looking at the values of n_0 along with the corresponding confidence intervals, it is possible to say that the light gases (CH₄ included) are basically characterized by n_0 values pretty close to the unity, with the exception of H₂, for which,

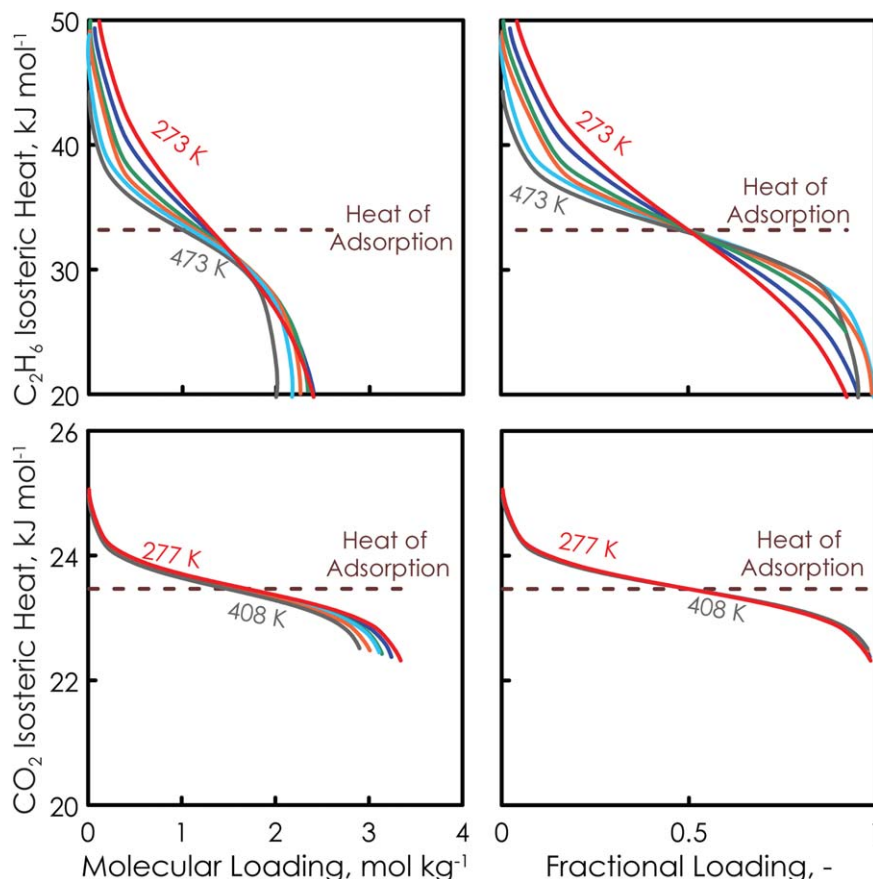


Figure 3. (a) Isosteric heat of adsorption of C_2H_6 vs. loading at (red line) 277 K, (blue line) 296 K, (green line) 338 K, (orange line) 373 K, (sky blue line) 408 K, (gray line) 473 K, and (b) isosteric heat of adsorption of CO_2 vs. loading.

[Color figure can be viewed in the online issue, which is available at wileyonlinelibrary.com.]

however, the calculation uncertainty is relatively higher than the others. This means that both Langmuir and Sips models provide very similar results and, thus, the former is able to describe the light gas behavior in the whole temperature range (weak lateral interactions). As for α , its vicinity to zero (even for N_2) confirm that, practically, the saturation loading of the light gases considered does not depend on temperature.

Differently, considering the hydrocarbons (CH_4 excluded), we can observe that the deviation from the Langmuir-type behavior is appreciable (n_0 sensibly different from the unity), this implying stronger lateral interactions. From a physical point of view, this is convincing because the longer the hydrocarbon chain, the stronger the molecule-molecule interactions, but it is not possible to observe a clear trend, as the n -butane shows a lower value of n_0 than propane.

However, it must be considered that the relative lower value of R^2 and the relatively wide confidence intervals do not allow to withdraw a clear conclusion about it. The same holds for the parameter α . Therefore, in order to check this and other possible peculiar trends, the whole temperature range was split into two consecutive subranges, whose results are shown and discussed in the next section.

Estimation of adsorption parameters:

Low- and high-temperature range

The temperature range is split into low and high temperature for all species but H_2 and CO , for which the low number

of available experimental isotherms is not sufficiently high to justify the split.

As for the Langmuir model, the R^2 values relative to the low-temperature range (Figure 4) are generally lower than those of the whole temperature range (Figure 1), which in turn is lower than the high-temperature one (Figure 5). At a first reading, this could be a “strange” finding, as the number of isotherms is less than before with the same number of parameters (four). However, this can be well understood if considering that the Langmuir model works slightly worse at low temperature for all the considered species, this effect being magnified for hydrocarbons. This means that the low-temperature hydrocarbons-zeolite interactions are not adequately described by the Langmuir model.

Analyzing the values of the single parameters, focusing on the saturation loading, it is possible to observe that all the considered hydrocarbons (CH_4 included) present values that decrease with increasing molecular weight, this being in line with the physical fact that the bigger the molecule, the smaller the available maximum loading.

Differently, the isosteric heat of adsorption of these hydrocarbons shows the opposite trend within all the temperature ranges considered. This indicates that the molecule-zeolite interactions become stronger for larger molecules, which is convincing from a physical point of view.

As for the temperature dependency of the saturation loading, given by the empirical parameter χ , there is an appreciable difference between low-, high-, and whole temperature range,

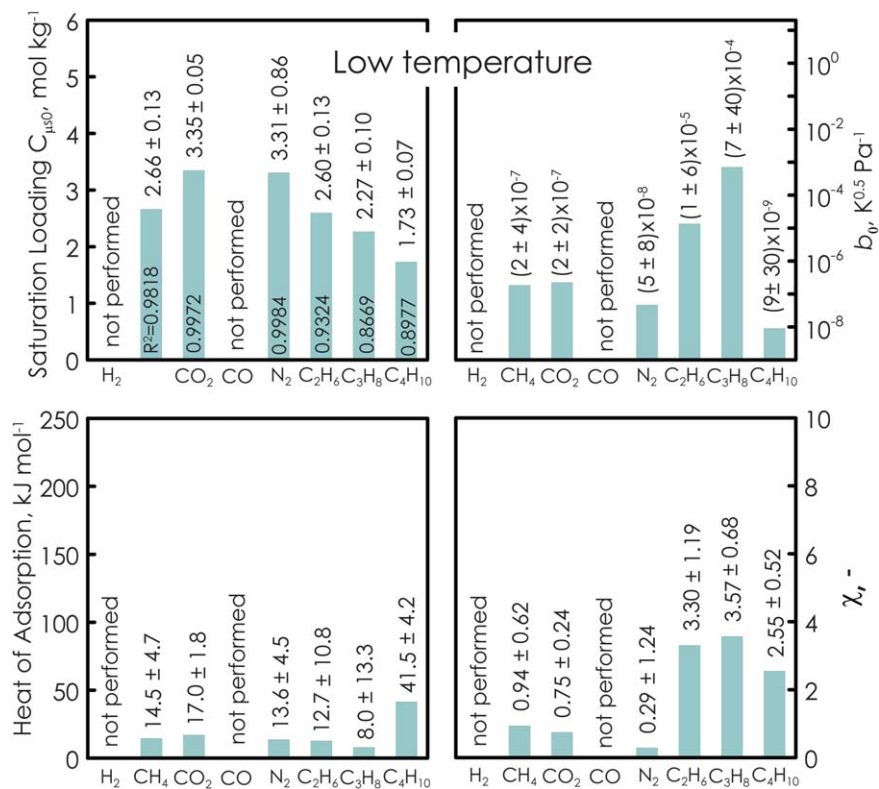


Figure 4. Calculated optimal values of the Langmuir model for the considered species.

Saturation loading $C_{\mu s0}$, parameter b_0 , isosteric heat of adsorption $Q_{\text{Ads,Lang}}$, empirical parameter χ_r . Low-temperature range (see Table 1). [Color figure can be viewed in the online issue, which is available at wileyonlinelibrary.com.]

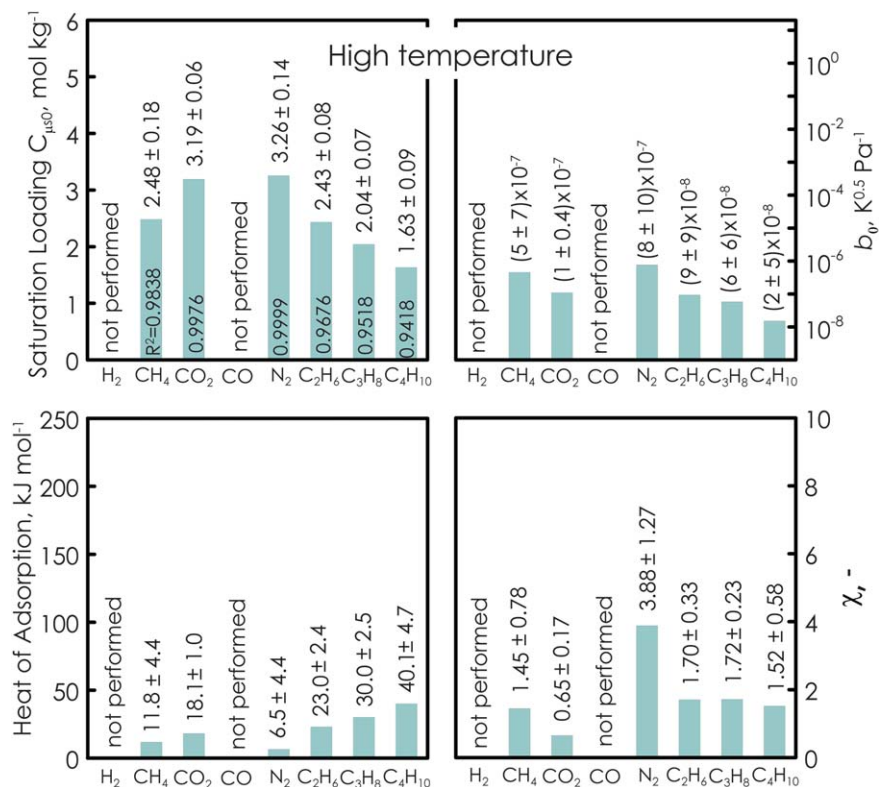


Figure 5. Calculated optimal values of the Langmuir model for the considered species.

Saturation loading $C_{\mu s0}$, parameter b_0 , isosteric heat of adsorption $Q_{\text{Ads,Lang}}$, empirical parameter χ_r . High-temperature range (see Table 1). [Color figure can be viewed in the online issue, which is available at wileyonlinelibrary.com.]

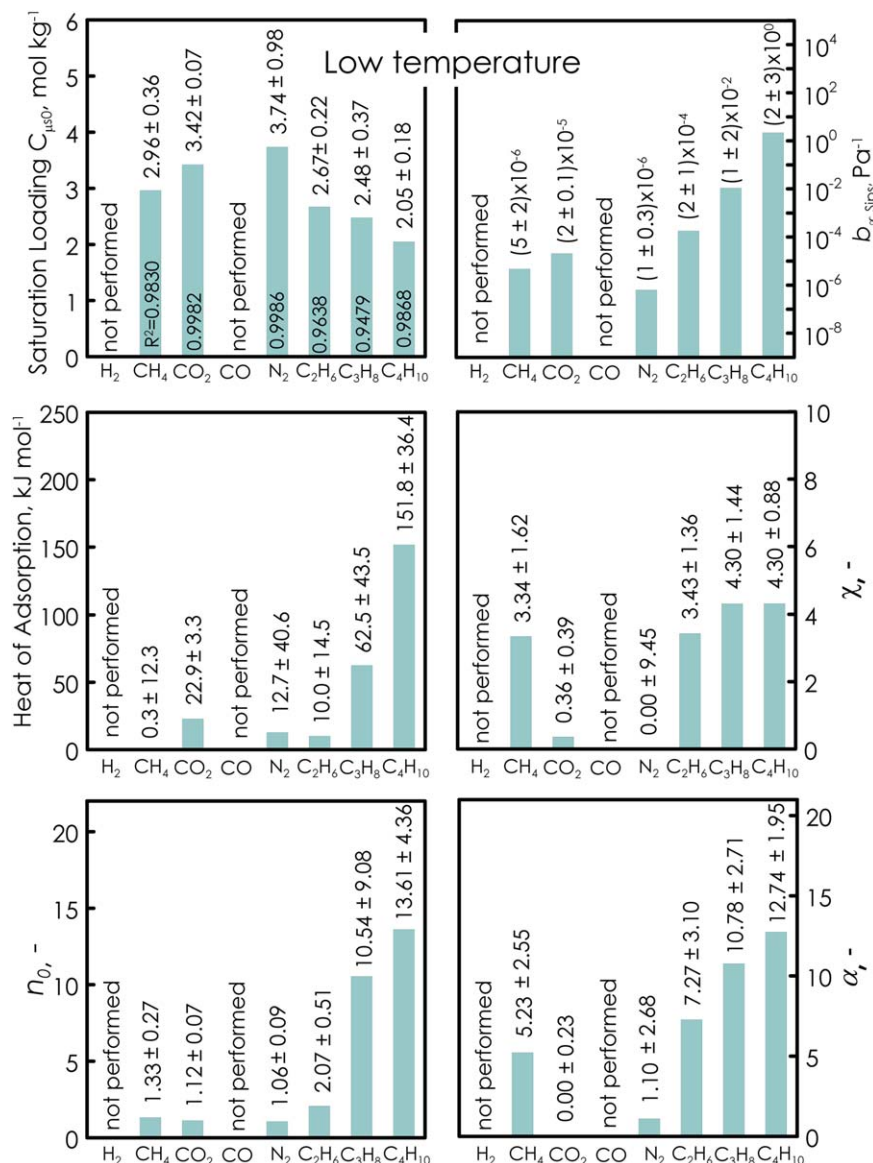


Figure 6. Calculated optimal values of the Sips model for the considered species.

Saturation loading $C_{\mu s0}$, Sips affinity constant at infinite temperature $b_{\infty,Sips}$, heat of adsorption $Q_{Ads,Sips}$, empirical parameter χ , empirical exponent n_0 , empirical parameter α . Low-temperature range (see Table 1). [Color figure can be viewed in the online issue, which is available at wileyonlinelibrary.com.]

although the R^2 values are comparable. The fact that the values of the parameters indicating the zeolite-molecule and the molecule-molecule interactions are lower at higher temperatures is physically convincing, as a higher temperature makes the adsorption strength weaker.

To choose the most convenient temperature range in the case where similar R^2 value is found, the criterion of the narrower confidence intervals can be used. Hence, based on this criterion and on the results shown in Figures 1, 4, and 5, we suggest that the readers use the values read from the results of the whole temperature range. Saturation loading, heat of adsorption, and the parameter χ show similar trend for both models (Figures 6 and 7).

Concerning the low-temperature range, it is possible to observe higher R^2 values with respect to the values of the Langmuir model, they being for some species even higher than the values calculated from the whole temperature range.

As for the light gases (CH₄, CO₂, and N₂), the R^2 values are basically pretty close to the unity and are almost the same in

all the temperature ranges considered. This means that the adsorption properties calculated from the whole temperature range are sufficiently accurate to be used at both low and high temperature.

Concerning the hydrocarbons (C₂H₆, C₃H₈, and C₄H₁₀), the first two have almost the same R^2 values in both the low-temperature range and the whole temperature range (0.96 and 0.94), while those in the high-temperature range are higher (0.98 and 0.96). This means that it is effective to split the whole range into low- and high-temperature range.

As for C₄H₁₀, the splitting convenience is even higher, as the difference among the three temperature ranges is larger. Such a convenience can be better understood if considering the previous discussion about the value of n_0 and α for hydrocarbons (CH₄ excluded). In fact, as for the n_0 , it is first confirmed that the lateral interaction between the light gases (CH₄ included) can be neglected in the adsorption process. Then, regarding the hydrocarbons, in both temperature trends are observed ranges for which n_0 increases with increasing hydrocarbon chain

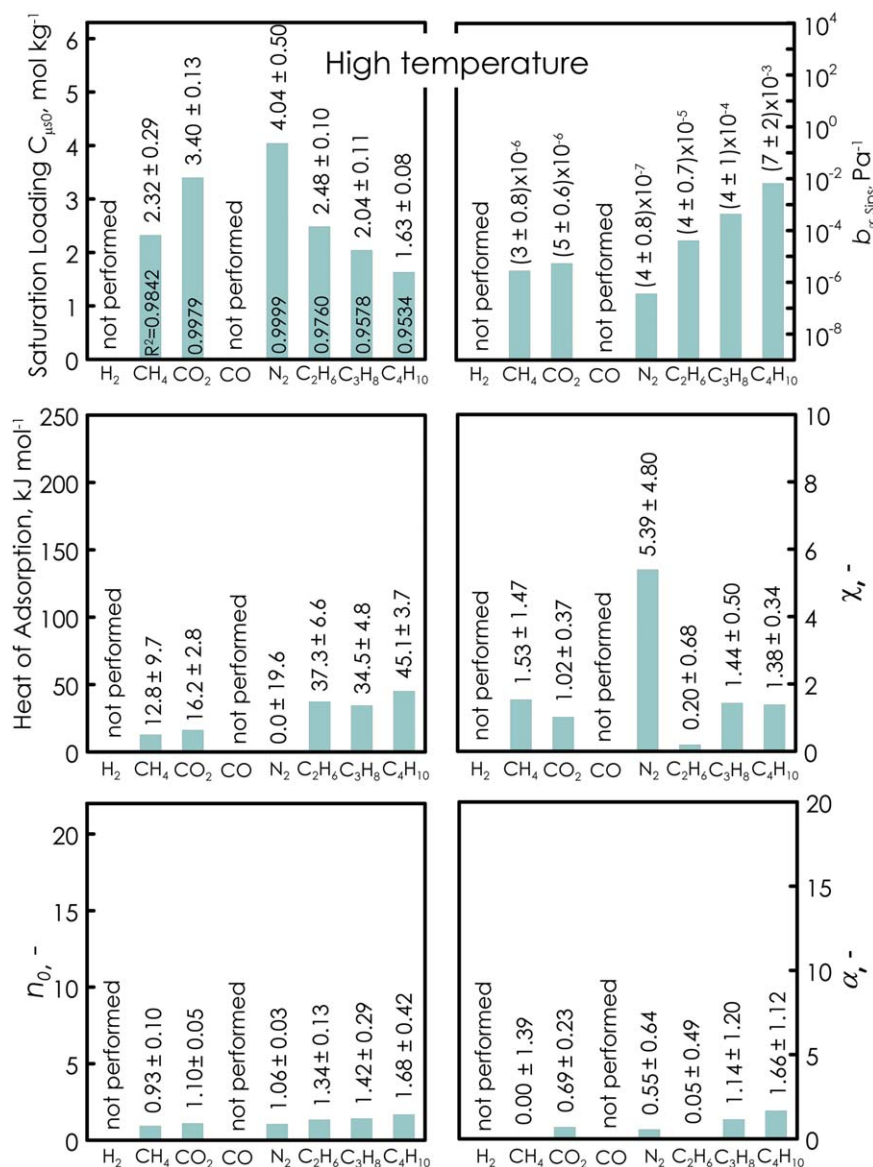


Figure 7. Calculated optimal values of the Sips model for the considered species.

Saturation loading $C_{\mu s0}$, Sips affinity constant at infinite temperature $b_{\infty,Sips}$, heat of adsorption $Q_{Ads,Sips}$, empirical parameter χ , empirical exponent n_0 , empirical parameter α . High-temperature range (see Table 1). [Color figure can be viewed in the online issue, which is available at wileyonlinelibrary.com.]

length, even though the uncertainty degree and the low determination coefficient of the propane calculation at low temperature could make doubts arise on the result reliability.

Nevertheless, we are convinced that this result is more reliable than that obtained from considering the whole temperature range, because the qualitative trend of n_0 observed in the low-temperature range is also found in the high-temperature one with even a higher degree of confidence. Furthermore, the fact that the values of the parameters n_0 and α calculated in the high-temperature range are significantly lower than those calculated in the low-temperature one has a precise physical meaning, that is, the influence of the lateral interactions decreases with increasing temperature (lower n_0), decreasing as well the functionality of the interactions with temperature (lower α).

Overall comparison with the literature

Before comparing the results arising from the two models, it is necessary to specify the significance given in this article to parity plots like Figures 8 and 9.

In general, this type of figures is made to compare the results of a model with those of experimental analysis. In doing that, the more the obtained results are close to the 45° line, the better the considered model reproduces the experimental behavior.

In this work, however, the parity plots in Figures 8 and 9 have to be read in a different way. In fact, in the hypothetical limit case in which the literature data laid along the 45° line, it would mean that our regression analysis provide the same results as those of the literature and that all literature data would be coherent to each other. In that case, our work would simply indicate that the model considered is fully able to reproduce the experimental behavior.

Conversely, if the results were far from the 45° line, it would mean that the literature data are not fully coherent to each other and that their global reconciliation is more difficult or, dually, that the reconciliation error is relatively high. In that case, the choice of the data suitable for regression would be crucial for obtaining meaningful results, as not all data could be reconciled.

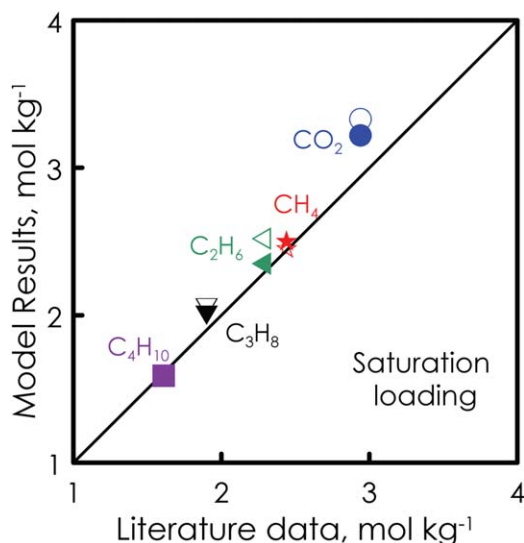


Figure 8. Comparison between saturation loadings evaluated in this work and some literature data for (☆, ★) CH_4 ,⁶ (○, ●) CO_2 ,²² (◁, ▷) C_2H_6 ,²³ (▽, ▼) C_3H_8 ,²⁴ (◻, ◼) C_4H_{10} .²⁴

Filled symbol for the Langmuir model and empty symbols for the Sips one. The data are calculated using the respective temperature values reported in each literature work. The data of CO and N_2 are not reported owing to discrepancies among the literature data.^{20,24} See Table 2 for a more complete comparison with the literature data. [Color figure can be viewed in the online issue, which is available at wileyonlinelibrary.com.]

To this regard, in this work we chose to exclude those data (i.e., isotherms) that are not coherent with the majority of the available data using the criterion explained above at the end of Introduction Section.

Moreover, the reconciliation presented in this article could also represent a reference point providing a useful indication for research groups fabricating zeolites, as they could relate and compare the properties of their specific zeolites to the literature. This aspect is even more important if considering that a number of researchers has been trying to improve the adsorption properties and increase the selectivity of the origi-

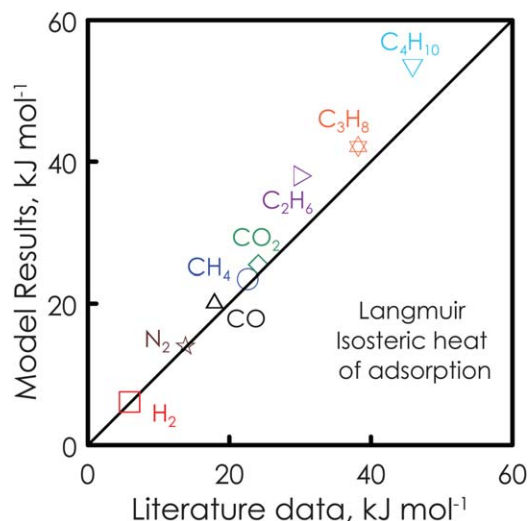


Figure 9. Comparison between the Langmuir isosteric heats of adsorption evaluated in this work and some values from the literature for (◻) H_2 ,²⁰ (○) CH_4 ,²⁰ (◊) CO_2 ,²⁰ (△) CO ,²⁰ (☆) N_2 ,²⁰ (▷) C_2H_6 ,²⁰ (☆) C_3H_8 ,²⁰ (▽) C_4H_{10} .²⁰

See Table 4 for a more complete comparison with the literature data. [Color figure can be viewed in the online issue, which is available at wileyonlinelibrary.com.]

nal zeolites by doping their structures with different type of ions.

Concerning the obtained results, the evaluated saturation loadings are coupled with some values from literature at different temperatures (Table 2 and Figure 8).

As partially shown in Table 2, the saturation loadings used in the literature are quite different from each other.^{6,10,20,22–25}

Table 3 reports the behavior of saturation loading with temperature for Langmuir and Sips models. As the magnitude of empirical parameter χ provides the temperature dependence of the saturation loading, saturation loadings evaluated for CO_2 , N_2 , C_2H_6 , and C_3H_8 with the Langmuir model have stronger temperature dependence than those evaluated with the Sips one.

Table 2. Comparison Between Saturation Loadings Evaluated in This Work and Some from Literature

Species	Langmuir $C_{\mu\text{s}}$ (mol kg ⁻¹)	Sips $C_{\mu\text{s}}$ (mol kg ⁻¹)	Literature $C_{\mu\text{s}}$ (mol kg ⁻¹)	Temperature (K)	References
H_2	1.96	0.71 (200 K)	5.4	200–290	20
CH_4	2.51	2.46	3.30	295	22
	2.50	2.45	2.44	296	24
	2.45	2.39	2.24	303	6
	2.45 (303 K)	2.39 (303 K)	2.69	303–408	10
CO_2	3.23	3.33	5.44	295	22
	3.22	3.33	2.94	296	24
	3.18	3.30	2.48	303	23
	3.18 (303 K)	3.30 (303 K)	2.97	303–408	10
CO	2.27	2.26	1.35	296	24
N_2	3.30	3.68	1.69	296	24
			5.4	200–320	20
C_2H_6	2.35	2.52	2.27	295	22
	2.27	2.50	1.85	303	6
C_3H_8	2.01	2.06	2.18	295	22
	2.00	2.05	1.90	296	24
C_4H_{10}	1.59	1.60	2.17	295	22
	1.59	1.59	1.61	296	24

Table 3. Saturation Loadings of the Langmuir and Sips Models with Increasing Temperature

Species	Temperature (K)	Langmuir $C_{\mu s}$ (mol kg ⁻¹)	Sips $C_{\mu s}^{-1}$ (mol kg ⁻¹)
H ₂	303	1.96	0.38
	323	1.96	0.34
	373	1.96	0.25
CH ₄	303	2.45	2.39
	323	2.30	2.21
	373	1.98	1.82
CO ₂	303	3.18	3.30
	323	3.06	3.24
	373	2.78	3.08
CO	303	2.24	2.22
	323	2.13	2.11
	373	1.89	1.86
N ₂	303	3.29	3.68
	323	3.28	3.68
	373	3.24	3.68
C ₂ H ₆	303	2.27	2.50
	323	2.07	2.43
	373	1.65	2.28
C ₃ H ₈	303	1.92	1.99
	323	1.73	1.83
	373	1.31	1.48
C ₄ H ₁₀	303	1.54	1.55
	323	1.42	1.43
	373	1.15	1.18

As for H₂ and CH₄, the saturation loading of CH₄ shows a stronger temperature dependence than that of H₂. Finally, in the case of CO and *n*-C₄H₁₀, the two models show the same temperature dependence of saturation loading.

In Table 4 and Figure 9, the Langmuir and Sips isosteric heat of adsorption of each component is compared with some literature values. The only difference between the estimated isosteric heats of adsorption and the literature data is in the pre-exponential factor of Eq. 2.

For the comparison, the expression of the Langmuir isosteric heat of adsorption (Eq. 11) is averaged over appropriate ranges of temperature and loading excluding the first term (Eq. 14) for the reasons explained above

$$Q_{\text{Iso,Lang}} = Q_{\text{Ads,Lang}} + \frac{\chi R_g T^2}{T_0(1-\theta)} \quad (14)$$

The general average expression valid for both models over appropriate ranges of temperature and fractional loading is the following

$$\bar{Q}_{\text{Iso}} = \frac{1}{T_b - T_a} \frac{1}{\theta_b - \theta_a} \int_{T_a}^{T_b} \int_{\theta_a}^{\theta_b} Q_{\text{Iso}} dT d\theta \quad (15)$$

Using Eq. 14 into Eq. 15, the following expression is obtained for the average isosteric heat of adsorption

$$\bar{Q}_{\text{Iso,Lang}} = Q_{\text{Ads,Lang}} - \frac{\chi R_g (T_a^2 + T_a T_b + T_b^2)}{3T_0} \ln \left(\frac{1-\theta_b}{1-\theta_a} \right) \quad (16)$$

A temperature range of 250–500 K and saturation loading between 0 and 0.9 were considered.

As can be observed in Figure 9, in this case, a very good agreement between evaluated values and literature data is obtained, this further confirming the validity of our approach. For CH₄, CO₂, C₂H₆, and N₂, isosteric heat of adsorption is also evaluated experimentally at different temperatures by

Table 4. Langmuir Isosteric Heats of Adsorption Compared with Some Values from Literature

Species	Isosteric Heat of Adsorption (kJ mol ⁻¹)		
	Present Work	Literature	References
H ₂	6.1	5.9	20
CH ₄	23.4	6.0	11
		23.3	10
		18.6	11
		22.6	20
CO ₂	25.4	21.1 (at 296 K)	15
		25.0	10
		24.1	11,20
		27.7 (at 304 K)	15
CO	20.1	17.9	20
		16.6	11
		13.8	20
N ₂	14.0	15.1	11
		17.7 (at 296 K)	15
		30.4	20
C ₂ H ₆	38.0	31.8 (at 296 K)	15
C ₃ H ₈	42.1	38.2	20
C ₄ H ₁₀	53.2	45.9	20

Dunne et al.¹⁵ The complete results obtained from this investigation can be found in Supporting Information.

Conclusions

The adsorption properties of various gases (H₂, CH₄, CO₂, CO, N₂, C₂H₆, C₃H₈, and C₄H₁₀) on silicalite were evaluated in terms of both Langmuir and Sips model parameters.

The calculation performed by considering three temperature ranges—namely low-, high-, and whole temperature range—allowed a clear identification of the effect of temperature on the model parameters, as well as the ranges where the two models work better.

As main results, the functionality of the adsorption parameters with temperature was achieved, this allowing a direct use of the obtained data for design purposes. Furthermore, based on the *R*² values, it was found that the Langmuir model works satisfactorily well in the whole temperature range (no need to split the calculation into different temperature ranges) for the light gases considered (CH₄ included) but not for the other hydrocarbons (C₂H₆, C₃H₈, and C₄H₁₀), for which it was found to be better to use the Sips model and split the temperature range using different adsorption parameters at low and high temperature, respectively.

The saturation loadings of the light gases evaluated with the Langmuir model in the whole temperature range were found to be weakly dependent on temperature for all the considered species, especially H₂. A slightly different trend was observed calculating the saturation loadings by the Sips model in the three temperature ranges considered. In this case, there is no clear tendency concerning the influence of temperature on the light gases saturation loadings, whose values were suggested to be read from low- and high-temperature range based on the temperature of interest of the end-users.

Acknowledgment

This project has received funding from the European Union through Seventh Programme for research, technological development and demonstration under grant agreement n. NMP3-LA-2011–262840 “DEMCAMER – Design and



Notation

- a = sticking coefficient
 b_{Lang} = Langmuir affinity constant, Pa^{-1}
 b_{Sips} = Sips affinity constant, Pa^{-1}
 b_0 = parameters in Eq. 4, $\text{K}^{0.5} \text{Pa}^{-1}$
 $b_{\infty, \text{Lang}}$ = Langmuir affinity constant at infinite temperature, Pa^{-1}
 $b_{0, \text{Sips}}$ = Sips affinity constant, Pa^{-1}
 $b_{\infty, \text{Sips}}$ = Sips affinity constant at infinite temperature, Pa^{-1}
 C_{μ} = molecular loading, mol kg^{-1}
 $C_{\mu s}$ = saturation molecular loading, mol kg^{-1}
 $C_{\mu s 0}$ = saturation molecular loading at the reference temperature, mol kg^{-1}
 $k_{d\infty}$ = desorption rate constant at infinite temperature, $\text{mol s}^{-1} \text{m}^{-2}$
 M = molar mass, kg mol^{-1}
 N = empirical exponent in the Sips model
 n_0 = empirical exponent in the Sips model at the reference temperature
 P = pressure, Pa
 Q_{iso} = isosteric heat of adsorption heat, J mol^{-1}
 Q_{Ads} = heat of adsorption heat, J mol^{-1}
 R_g = gas constant, $8.314 \text{ J mol}^{-1} \text{K}^{-1}$
 T = temperature, K
 T_0 = reference temperature, K

Greek letters

- α = empirical parameter in Eq. 8
 χ = empirical parameter in Eq. 9

Literature Cited

- Do DD. Adsorption Analysis: Equilibria and Kinetics. London: Imperial College Press, 1998. ISBN 1-86094-137-3.
- Tavolaro A, Drioli E. Zeolite membranes. *Adv Mater.* 1999;11:975–996.
- Baerlocher C, McCusker LB, Olson DH. Atlas of Zeolite Framework Types, 6th revised ed. Amsterdam: Elsevier, 2007.
- Himeno S, Takenaka M, Shimura S. Light gas adsorption of all-silica DDR- and MFI-type zeolite: computational and experimental investigation. *Mol Simul.* 2008;34:1329–1336.
- Diaz I, Kokkoli E, Terasaki O, Tsapatsis M. Surface structure of zeolite (MFI) crystals. *Chem Mater.* 2004;16:5226–5232.
- Zhu W, van de Graaf JM, van den Broeke JP, Kapteijn F, Moulijn JA. TEOM: a unique technique for measuring adsorption properties. Light alkanes in silicalite-1. *Ind Eng Chem Res.* 1998;37:1934–1942.
- Richards RE, Rees LVC. Sorption and packing of n-alkane molecules in ZSM-5. *Langmuir.* 1987;3:335–340.
- Algieri C, Barbieri G, Drioli E. Zeolite membranes for gas separations. In: Drioli E, Barbieri G, editors. *Membrane Engineering for the Treatment of gases. Volume 2: Gas-Separation Problems Combined with Membrane Reactors, Chapter 17.* Cambridge, England: RSC publishing, 2011:223–252.
- Lovaglio MC, Gouzinis A, Tsapatsis M. Synthesis and characterization of oriented MFI membranes prepared by secondary growth. *AIChE J.* 1998;44:1903–1913.
- Zhu W, Hrabanek P, Gora L, Kapteijn F, Moulijn JA. Role of adsorption in the permeation of CH_4 and CO_2 through a silicalite-1 membrane. *Ind Eng Chem Res.* 2006;45:767–776.
- Golden TC, Sircar S. Gas adsorption on silicalite. *J Colloid Interface Sci.* 1994;162:182–188.
- Sun MS, Shah DB, Xu HH, Talu O. Adsorption equilibria of C_1 to C_4 alkanes, CO_2 , and SF_6 on silicalite. *J Phys Chem B.* 1998;102:1466–1473.
- Abdul-Rehman HB, Hasanain MA, Loughlin KF. Quaternary, ternary, binary, and pure component sorption on zeolites. 1. Light alkanes on linde S-115 silicalite at moderate to high pressures. *Ind Eng Chem Res.* 1990;29:1525–1535.
- Hampson JA, Rees LVC. Adsorption of ethane and propane in silicalite-1 and zeolite NaY: determination of single components, mixture and partial adsorption data using an isosteric system. *J Chem Soc Faraday Trans.* 1993;89(16):3169–3176.
- Dunne JA, Mariwala R, Rao M, Sircar S, Gorte RJ, Myers AL. Calorimetric heats of adsorption and adsorption isotherms. 1. O_2 , N_2 , Ar, CO_2 , CH_4 , C_2H_6 , and SF_6 on silicalite. *Langmuir.* 1996;12:5888–5895.
- Zhu W, Kapteijn F, Moulijn JA. Equilibrium adsorption of light alkanes in silicalite-1 by the inertial microbalance technique. *Adsorption.* 2000;6:159–167.
- Wirawan SK, Creaser D. CO_2 adsorption on silicalite-1 and cation exchanged ZSM-5 zeolites using a step change response method. *Microporous Mesoporous Mater.* 2006;91:196–205.
- Yang J, Li J, Wang W, Li L, Li J. Adsorption of CO_2 , CH_4 , and N_2 on 8-, 10-, and 12-membered ring hydrophobic microporous high-silica zeolites: DDR, silicalite-1, and beta. *Ind Eng Chem Res.* 2013;52:17856–17864.
- Caravella A, Zito PF, Brunetti A, Drioli E, Barbieri G. Adsorption properties and permeation performances of DD3R zeolite membranes. *Chem Eng Trans.* 2015;43:1075–1080.
- Bakker WJW, van den Broeke LJP, Kapteijn F, Moulijn JA. Temperature dependence of one-component permeation through a silicalite-1 membrane. *AIChE J.* 1997;43:2203–2214.
- Available at <http://www.mathworks.it/help/optim/ug/lsqcurvefit.html>.
- Bakker WJW, Kapteijn F, Poppe J, Moulijn JA. Permeation characteristics of a metal-supported silicalite-1 zeolite membrane. *J Memb Sci.* 1996;117:57–78.
- Van den Broeke LJP, Bakker WJW, Kapteijn F, Moulijn JA. Transport and separation properties of a silicalite-1 membrane-I. Operating conditions. *Chem Eng Sci.* 1999;54:245–258.
- Otto K, Montreuil CN, Todor O, McCabe RW, Gandhi HS. Adsorption of hydrocarbons and other exhaust components on silicalite. *Ind Eng Chem Res.* 1991;30:2333–2340.
- Lee SC. Prediction of permeation behavior of CO_2 and CH_4 through silicalite-1 membranes in single-component or binary mixture systems using occupancy-dependent Maxwell-Stefan diffusivities. *J Memb Sci.* 2007;306:267–276.

Manuscript received Dec. 22, 2014, and revision received May 11, 2015.